Journal of Achievements in Materials and Manufacturing Engineering

VOLUME 46
ISSUE 1
May
2011

# Relationship between geometric welding parameters and optical-acoustic emissions from electric arc in GMAW-S process

**E. Huanca Cayo*, S.C. Absi Alfaro**
Mechanical/Mechatronic Engineering Department, University of Brasilia, Campus Universitário Darcy Ribeiro - Asa Norte 70.910-900, Brasilia - DF - Brazil
* Corresponding author: E-mail address: eber@unb.br

Received 02.04.2011; published in revised form 01.05.2011

**Manufacturing and processing**

## ABSTRACT

**Purpose:** Show the relationship between geometric characteristics of the weld bead and the optical-acoustic emissions from electric arc during welding in the GMAW-S process.

**Design/methodology/approach:** Bead on plate welding experiments was carried out setting different process parameters. Every welding parameter group was set aiming to reach a high stability level what guarantee a geometrical uniformity in the weld beads. In each experiment was simultaneously acquired arc voltage, welding current, infrared and acoustic emissions; from them were computed parameters as arc power, acoustic peaks rate and infrared radiation rate. It was used a tri-dimensional LASER scanner for to acquire geometrical information from the weld beads surface as width and height of the bead. Depth penetration was measured from sectional cross cutting of weld beads.

**Findings:** Previous analysis showed that the arc emission parameters reach a stationary state with different characteristic for each experiment group which means that there is some correlation level between them. Posterior analysis showed that from infrared parameter is possible to monitoring external weld bead geometry and principally its penetration depth. From acoustic parameter is possible to monitoring principally the external weld bead geometry. Therefore is concluded that there is a close relation between the arc emissions and the weld bead geometry and that them could be used to measuring the welding geometrical parameters.

**Research limitations/implications:** After analysis it was noticed that the infrared sensing has a better performance than acoustic sensing in the depth penetration monitoring. Infrared sensing also sources some information about external geometric parameters that in conjunction with the acoustic sensing is possible to have reliable information about weld bead geometry. This method of sensing geometric parameters could be applied in other welding processes, but is necessary to have visibility of the arc, it means that for example this method cannot be used in the submerged arc welding - SAW process.

**Originality/value:** The using two or more sensors for monitoring welding parameters increases the performance and reliability of the measurements. In this case, the monitoring of the weld bead geometric parameters could be possible from sensing arc emission and potentially it could be used as an on-line monitor, avoiding any complex electric connections of sensors into the welding process.

**Keywords:** Monitoring; Arc emissions; Geometrical parameters; Weld bead; GMAW-S

**Reference to this paper should be given in the following way:**
E. Huanca Cayo, S. C. Absi Alfaro, Relationship between geometric welding parameters and optical-acoustic emissions from electric arc in GMAW-S process, Journal of Achievements in Materials and Manufacturing Engineering 46/1 (2011) 79-87.

## 1. Introduction

Gas metal arc welding - GMAW in short circuit mode process (hereafter named as GMAW-S), is the manufacture process most used in the metallic construction industry. Diverse advantages such as the high rate metallic transference, elevated penetration and facility to welding in diverse positions, does this process become the most requested. When the GMAW-S process demand grew at industrial rates, its quality requirements and exigencies also were multiplied. Welding quality assessment is subject at multiple investigations and discussions, due to its qualification involve diverse criteria such as metallurgical and geometrical continuity throughout weld bead. The weld bead geometry is result of previous setting of welding parameters and its on-line monitoring is necessary for guarantying the welding quality. Classically are monitored arc tension and welding current.

These parameters are stability indicators of electric arc and also their behaviour have direct implications in the heat and metal transference which is reflected in the weld bead geometry. Besides classical parameters, during welding, the electric arc produces mechanical, optical and electromagnetic emissions. It is known that expert welders use some arc emissions as sound and luminosity for monitoring and controlling the welding process aiming to achieve high stability and quality. [1]. Different researches showed that is possible to detect some interference and to assess the welding quality by measuring the sound and optical emissions as infrared band [2-7]. Besides perturbations detection, it was also shown that from infrared emissions is possible to measure depth penetration. The goal of this paper is to show the relationships between acoustic and infrared arc emissions and geometric characteristics of the weld bead. In first time, was approached the relationships between direct and indirect welding parameters. Secondly it was described the methodology after was approached the results and finally the principal conclusions.

### 1.1. Relationships between direct and indirect welding parameters

The Figure 1 shows a classification of welding parameter resultant of conjunctions of different classifications reviewed [8]. The parameters were divided into direct (DWP) and indirect (IWP), which correspond at input and output parameters respectively. Within IWP, fix and adjustable parameters are set before start the welding process. Are named as fix parameters all previous characteristics of materials surrounded in welding, as well as the structural design and configuration of joint. Some adjustable parameters such as current and voltage waveform, contact distance tip to work piece (CTWD), wire feed speed and travel speed can be varied on-line during the process. This happens in feedback control welding process. The DWP is separate into weld bead parameters and arc welding phenomena. The first group is composed by parameters related at weld bead characteristic such as external geometry, depth penetration, reinforcement, fusion zone geometry, mechanical properties, microstructure, and discontinuities. The second group is composed by the arc welding emissions.

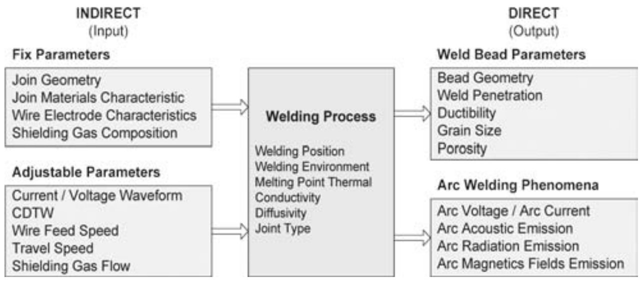


Fig. 1. Welding parameters classification

Figure 1 makes it clear that the welding process is a multi-input, multi-output (MIMO), multivariable system. Also, note that the relation between the input and output variables is dynamic, highly nonlinear, and strongly coupled. A schematic of the effect of some IWP on some DWP is shown in Figure 2 [9], where (+) indicates an increase is followed by an increase and (-) indicates an increase is followed by a decrease.

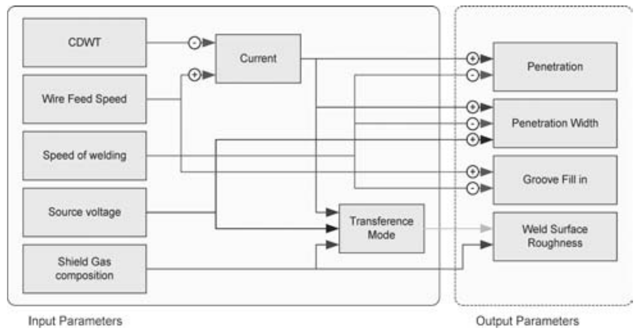


Fig. 2. Relationship between welding parameters in GMAW process

## 2. Experimental setup

A decibel meter and a pyrometer in the cases of acoustic and infrared emissions respectively were used. Their setups are showed in the Figure 3. The decibel meter B&K 2250 uses a 4189 type microphone with -26 ±1.5 dB gain, ±1.0 output amplitude signal and sensitivity of 50 V/Pa. This device was covered with a aluminium shell for protection against welding spatter. Studies in psychoacoustic have determined that if the electric arc sound signal does not exceed 400 ms, this will be a good indicator of the behaviour weld process [4]. Following these considerations, in this work the microphone was positioned at 200 mm from the arc. The pyrometer TL-S-25 has as output signal a current sign between 4-20 mA which is proportional to the registered temperature (measuring Range 800–2.500 °C). To locate the position of the sensor correctly (arc welding and weld pool), the TL-S-25 pattern provides a tool for localizing the best place for the temperature measurement. This tool is a laser incorporated into a sensor, which shows the focus; for this pattern the focus localization is 600 mm.

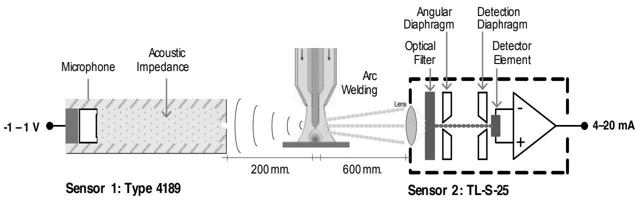


Fig. 3. Arc emission sensors

Virtual instrumentation software, data acquisition card, energy source and sensoring equipment set up as shown in the Figure 4 was used for acquisition and processing data based on the voltage, current, sound and infrared signals. Those signals were sampled at 20 kHz. The decibel meter B&K output signal (+/- 5V) was linked to acquisition card. The pyrometer output was converted from current (4-20 mA) to voltage (0-5V) using a current/voltage converter which also was finally linked to acquisition card. Arc voltage was acquired by a voltage shunt and optical insulator connected to acquisition card. The welding current was acquired by a Hall Effect sensor linked at acquisition card previously conditioned.

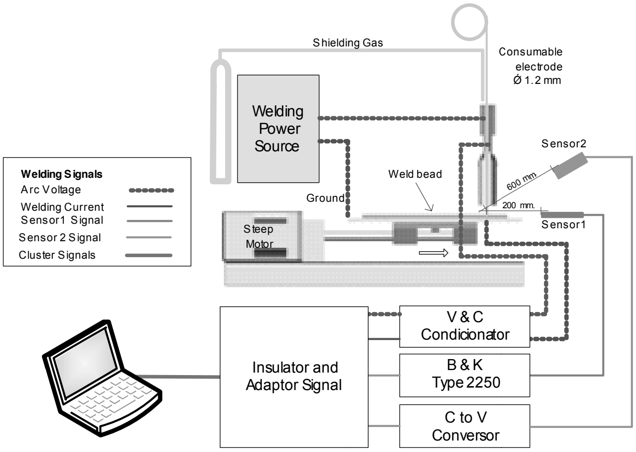


Fig. 4. Experimental setup

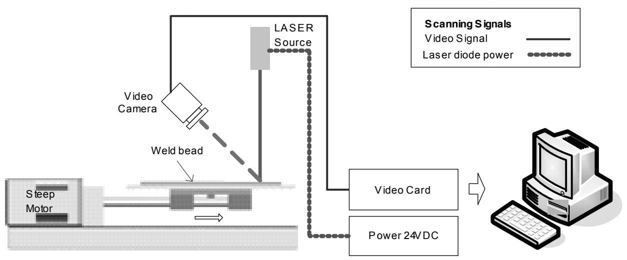


Fig. 5. Scanner setup

In the Figure 5 is showed the Laser scanner configuration for measuring the evolution of external weld bead geometrical parameters such as width, and height. This scanner is composed by a CCD camera and Laser flash line in tri-angled position. During scanning is recorded the weld profile video at 30 frames per second, focusing the laser line on the bead (which is the weld bead profile).

The welds were carried out on steel plates AISI 1020 (140 mm x 101.2 x 9.60 mm), electrode wire AWS A5.18 ER70S-6 with 1.2 mm of diameter, shield gas was the mixture of argon and carbonic anhydride M21 (ATAL 5A/Ar 82% + CO2 18%). The welding runs were performed keeping fixed contact tip work distance – CTWD at 10mm. and shield gas flow at 15 l/min. These experiments were executed setting combinations for four arc voltage levels (18, 19, 20 and 21 - V), five levels to wire feed speed (3.0, 3.5, 4.0, 4.5 and 5.0 - m/min) and three welding speed levels (7, 9 and 11 – mm/s) which in total are sixty welding experiments.

# 3. Results and Discussions

## 3.1. Geometrical Parameters

Two geometrical parameters were obtained from image processing software applied at recorded weld profile video (from scanner). The first step is processing the weld bead profile image frames consists in to transform the full colour image to gray scale. Secondly, on the gray scale image, was applied an edge filtering for obtaining the weld bead contour line. From the contour line, it was computed the width and height of weld bead (see Figure 6.a). Each video frame supplies geometrical set dimensions and for to have a general dimensional information from each weld bead, it was calculated the average for each using the equation (1). Depth penetration was measured from sectional cross cutting of each weld bead. Figure 6.b shows the depth penetration aspect.

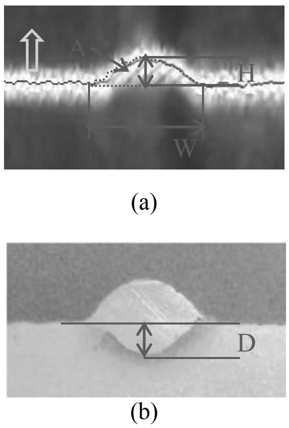


Fig. 6. Weld bead dimensions

$$\overline{D} = \frac{1}{n}\sum_{i=1}^{n} D_i = \frac{1}{n}(D_1 + ... + D_n) \quad (1)$$

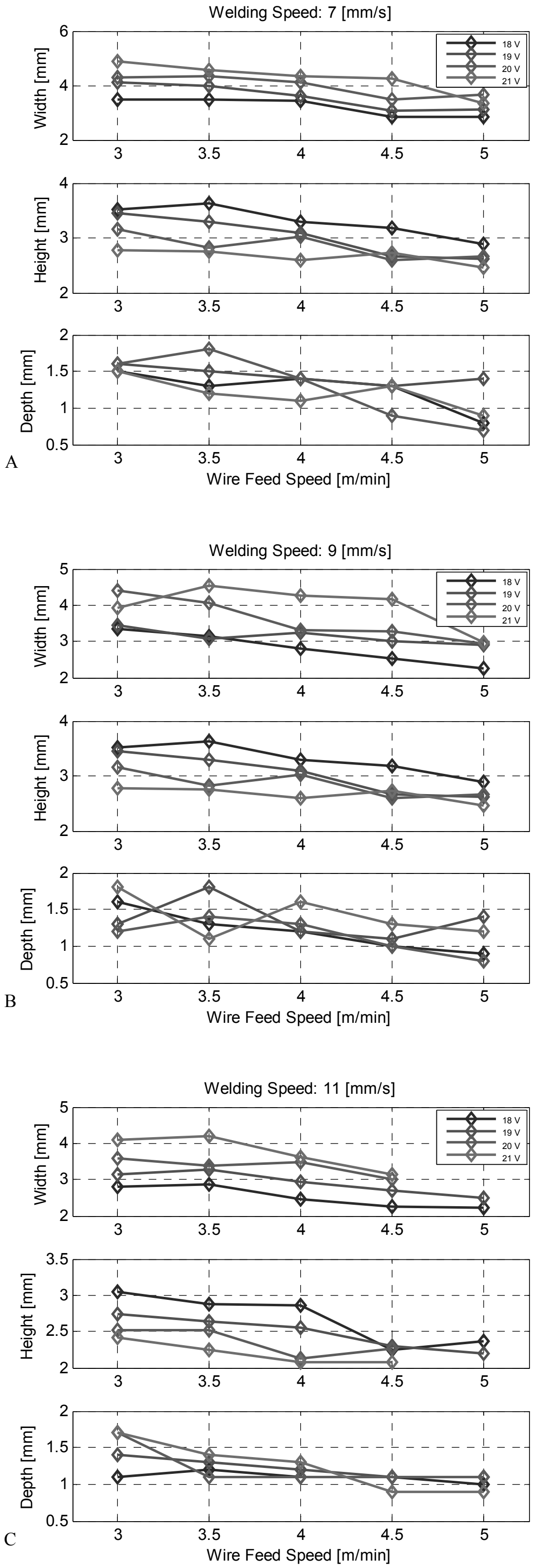


Fig. 7. Geometric parameters

Where, $\overline{D}$ is the average of the geometric parameter computed (it can be width, height or area),$D_i$ is the ith measured parameter, n is the total geometric data of each weld bead scanned.

After measuring the geometric parameters in the weld bead, we can to notice their relationships for each welding speed. Figures 7.a, b, and c represent the evolution of the geometrical parameters in four arc voltage levels for 7, 9 and 11 mm/s welding speed respectively. In all below graphs are noticed that there is inverse relationship between the arc voltage and the height of weld bead. Unlike height, the width and depth have a direct relationship with the arc voltage. This means that when the arc voltage increases, the width and depth also increase and the height decreases. This inverse proportion is similar for each welding speed. Also is noticed that when the welding speed increases, all geometrical parameters decrease in numerical terms; they decrease also when the wire feed speed increases. It has sense, because when the welding speed increases the time for transfer cycle is minor and so the metal transferred from wire tip to welding pool decreases when the welding speed increases. This fact gives origin at dimensional changes in each geometric parameter.

## 3.2. Arc Emissions

Figure 8 shows a data window of welding parameter signals monitored simultaneously, voltage and current (A), acoustic emission (B) and infrared emission (C).

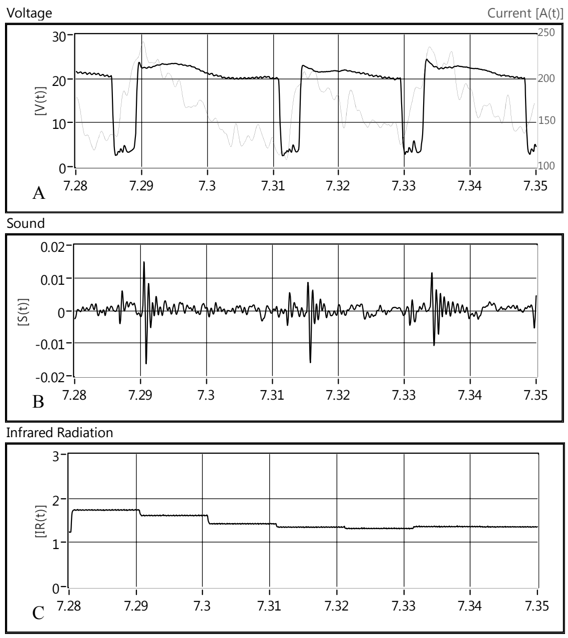


Fig. 8. Welding parameters

**ACOUSTIC EMISSIONS:**

The arc voltage is characterized by ignitions and extinction arc sequence cycles (A) and that the arc sound fit the arc voltage cycles. In every ignition of the arc voltage there is a big sound peak, whereas in every arc voltage extinction there is a small peak of sound (B). Also is noticed that there is a delay in the sound compared with the arc voltage. This delay is produced by the airborne nature of the sound and its value is not great than 400 ms, which means that the arc sound is feasible for to get reliable information from behaviour of the electric arc [4]. Researches on arc sound monitoring [2]-[4], describe that the relationship between the sound produced *S(t)* and the arc power *P(t)=V(t)I(t)·* can be expressed by equation 2.

$$S_c(t) = K\left[\frac{d(P(t))}{dt}\right] \tag{2}$$

$$K = \alpha(\gamma - 1)/c^2 \tag{3}$$

Where: $S_c(t)$ is the computed sound, K is a proportionality factor, α is a geometrical factor, γ the adiabatic expansion coefficient of air and the velocity of sound in the arc.

**INFRARED EMISSIONS:**

Figure 8 shows the infrared radiation response (D) and we can notice that this parameter does not fit the arc voltage behaviour but in later section it will be shown that it has a direct relation with arc power. Infrared emission is originated by the electromagnetic energy emitted for the welding electric arc and sensed just at infrared wavelength (0.8 - 1.1$\mu m$ specified in the pyrometer datasheet). Its intensity and wavelength of energy produced depend on the welding parameters, electrode and base metal composition as well as fluxes of shielding gas. Intensity of this electromagnetic emission is governed by Planck's law which describes the spectral radiance of unpolarized electromagnetic radiation at all wavelengths emitted from a black body at absolute temperature *T*. As a function of frequency *v*, Planck's law is written as:

$$I(v,T) = \frac{2hv^3}{c^2}\frac{1}{e^{\left[\frac{hv}{kT}\right]} - 1} \tag{4}$$

Where is also named as spectral radiance (J.m$^2$.sr$^{-1}$), T temperature (K) v frequency (Hz), h Plank constant (6.62606896(33) ×10 -34 J.s), speed of light (3.0 ×10 8.m/s) and k Boltzmann constant (≈ 1.3806504) ×10 -23 J/K).

Although stationarity of GMA welding process parameters [10] and similarity of the behaviour between the envelope of sound signal and the arc voltage and/or welding current as well as infrared emission, is necessary to show the stationarity of the acoustic and infrared emissions, because both emissions have not electric connections at welding process, and their characteristics could defer from welding parameters due to propagation way through environment what is subject at no linear possible variations originated by changes in the adiabatic expansion coefficient , variations in the sound speed by changes in the temperature of the air surround to arc welding pool as well as due to noise of the environment, shielding gas fluxes, etc. Determining the stationarity of arc emissions, will permit to these to be reliable parameters to monitoring the transfer cycles in GMAW-S process. In the next section will be analyzed their stationarity.

## 3.3. Stationarity of arc emissions

Stationarity is a statistical property of random nature processes what means that the statistical quantities are independent of the absolute time and dependant only on relative times, in other words a process is stationarity when its essential statistical properties are invariant over time. Two kinds of stationarity are distinguished: weak and strong stationarity. Weak stationarity is meant when the first and second moments are independent of time, that is, $\langle E_t \rangle = \mu$ and $\langle [E_t - \mu]^2 \rangle = \sigma^2$, (where $\langle \cdot \rangle$ stands for the ensemble average) are constants. For finite process which is the case of the welding processes, the behavior of the mean value and variance cannot be enough estimators for stationarity. A stochastic process with as an integer number, is denominated as strongly stationary if any set of times and any integer the joint probability distributions of $\{E_t, ..., E_{tn}\}$ and $\{E_{t_{1+k}} + E_{tn+k}\}$ coincide, in other words, when there is correlation between both distributions. Before to calculate the autocorrelation function is necessary obtain some statistical parameters considering some arc emission as a stochastic variable, $E(t,\beta)$.

Probability average

$$\langle E \rangle_j = \lim_{N\to\infty} \frac{1}{N}\left[\sum_{i=1}^{N} E(\beta_i, \tau_j)\right] \tag{5}$$

$j = 1,2,..., M+1$

Where: is the number of realizations of the process is the number of time steps and is the random variable.

Time Average

$$\bar{E} = \lim_{T\to\infty} \frac{1}{2T}\int_0^T E(t)dt \tag{6}$$

Fluctuations

$$E'(t) = E(t) - \bar{E} \tag{7}$$

Since $\overline{E'(t)} = 0$, the variance is simply calculated as:

$$\sigma_{s'}^2 = \overline{E'^2} \tag{8}$$

The time average of the square of the fluctuations is evaluated by using the expression in equation (9).

$$\overline{E'^2} = \lim_{T\to\infty} \frac{1}{N}\int_0^T E'^2(t)dt \tag{9}$$

Finally the autocorrelation is defined as:

$$R_{E'}(\tau) = \langle E'(t+\tau)E'(t) \rangle = \overline{E'(t+\tau)E'(t)} \tag{10}$$

It is more convenient to work with the normalized autocorrelation function $C_S$, defined in equation (11).

$$C_{E'}(\tau) = \frac{R_{E'}(\tau)}{\sqrt{\overline{E'^2(t)}}\sqrt{E'^2(t+\tau)}} \tag{11}$$

Note that indicates weak stationarity and $C_E=0$ indicates strong stationarity. Figure 9 (A) and (B) displays the plots of the normalized autocorrelation of acoustic and infrared emissions.

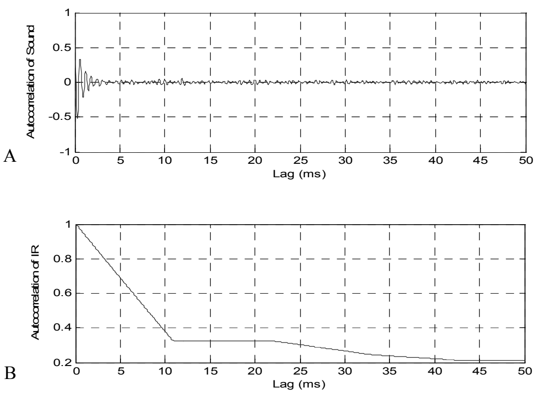


Fig. 9: Arc emissions correlation.

Generally, the autocorrelation is expected to decay exponentially, and the fluctuations are expected to become uncorrelated after a sufficiently long-time. From the graph in Figure 9 A and B, it is observed that there is a high autocorrelation what means that the acoustic and infrared emissions have a strong stationarity and it can be used to assessing as welding quality parameter. From arc emissions signals, were computed two arc emission parameters: ignition rate (IgR) from sound and infrared rate (IR) from infrared emission.

## 3.4. Emission Parameters

**IGNITION RATE:**

By applying a quadratic amplitude demodulation operator $H[\square^2]$ at arc sound signal, is calculated its envelope. From sound envelope is possible to notice pulses produced by short circuits and ignitions from arc what can be accounted and named as ignition rate (IgR). Figure 10 shows the ignition rate response when the arc welding power (root mean square) changes between two levels. Is possible to notice that they have inverse relation, it means that when arc power increases the ignition rate decreases. This happens due to the increase in power means increasing the transference rate which reduces the short circuit rate. Increasing power could change the transference way to globular or spray mode when there is not short circuits and the acoustic emission showing transference cycles would be null. This relation shows that is possible to measure and monitor welding power behaviour by acoustic emissions from arc in GMAW-S process.

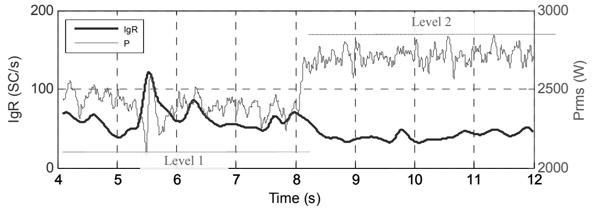


Fig. 10. Ignition rate and welding power

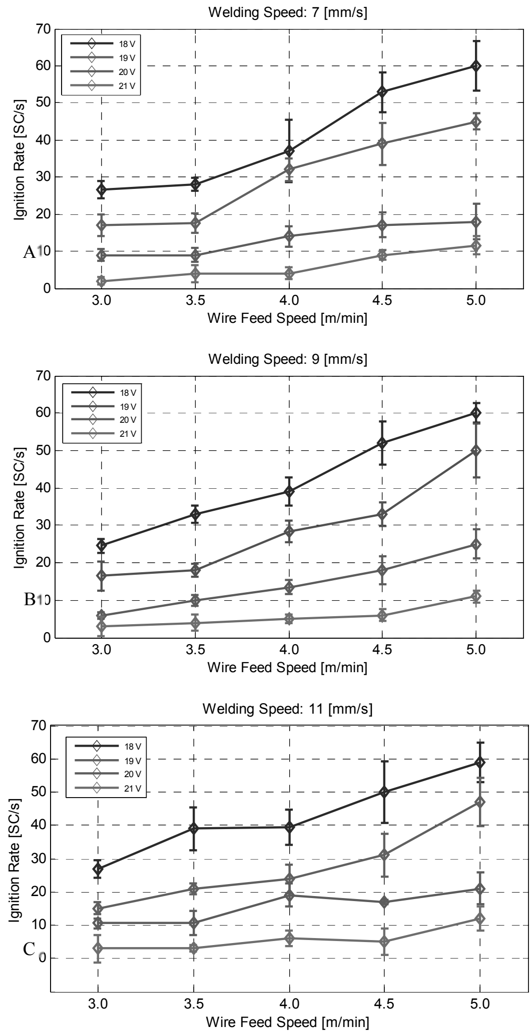


Fig. 11. Ignition rate

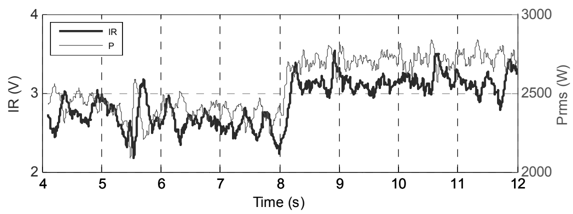


Fig. 12. Infrared rate and welding power

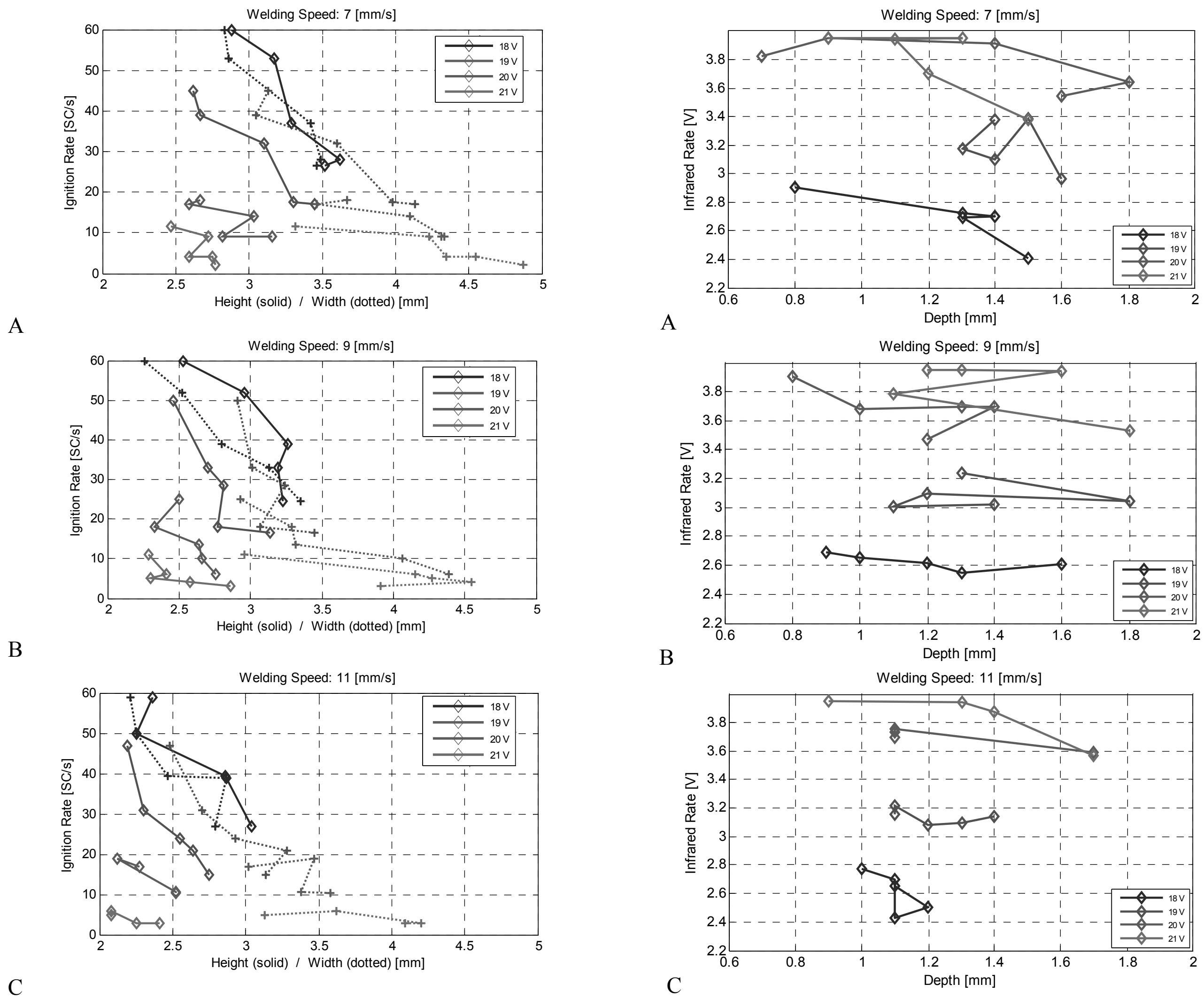


Fig. 14. Infrared emission and depth penetration

The distributions of ignition In the Figure 11 is shown the evolution for the ignition rate against wire feed speed for four arc voltage levels. Each graph (A, B and C) was plotted for welding speeds: 7, 9 and 11 mm/s respectively. rates have a progressive and continuous increase in function of wire feed speed for all welding speed rates. The proportionality between the short circuit rate and the wire feed speed is direct; it means that when increases one increase the other. This happens contrarily in the case of the arc voltage. When there are increases in arc voltage, the rate of short circuits decreases. We can notice also that the standard deviation is greater when the arc voltage increases.

**INFRAED RATE:**

As explained in section 3.2, the infrared radiation does not fit the sequence of short circuits and ignitions produced in the electric arc. Nevertheless, infrared emissions fits at arc power (root mean square) as is shown in Figure 12 where is possible to notice changes in two levels of arc power also fitted by infrared emission.

Figure 13. Acoustic emission and weld bead dimensions

Figures 13 - a, b and c, show the relationship between the average ignition rate and weld bead height (solid) and width (dotted) for 7, 9 and 11 mm/s welding speed respectively. From those graphs we can to notice that when increases the arc voltage, ignitions rate decreases as well as weld bead height but there is an inverse relationship with the weld bead width which decreases. When welding speed is increased the weld bead height and width decrease. In Figure 14 is shown the evolution of the depth penetration and how the infrared rate behaviour is for 7, 9 and 11 mm/s of welding speed. In all graphs is possible to notice that the infrared rate increases when the arc voltage is increased too. From all graphs, the weld beads performed with 11 mm/s show less variation on their responses and comparing it with their responses in ignition rate (Figure11), infrared emission rate (Figure 13) as well as with the weld bead geometry (Figure 7) we can notice that this welding set have more stability and better geometric uniformity.

Their performance can be noticed in their uniform distribution in the parameters described before in function of wire feed speed for welding speed 11 mm/s.

For this stable set (weld bead set performed at 11 mm/s), welding bead performed with 19 and 20 V have shown more stability.

This could be noticed that when the voltage exceeds 20 V, instabilities appear due to high welding current reduces the time transfer and it in combination with a slow wire feed speed could generates temporal instabilities, transfer mode changes till undesirable structural and geometric discontinuities. If the short-circuit current is too high, it has a considerable effect on the pinch-off forces, causing weld spatter. The power must be high enough to keep the temperature of the arc sufficient for the continued transport of the current and it can be monitored by infrared emissions. Current is set indirectly by the wire feed speed and as it is direct related at weld heat, it can reduce with welding speed. For arc voltage under 19 V, welding process also becomes instable due to low welding current which cannot to supply enough heat in the metal transfer, generating electrode wire explosions and insufficient depth penetration and an inacceptable quality in the weld bead. There are different characteristics of welding parameters to reach a high stability. It is reached in GMAW-S when the pool fusion oscillation and short circuit frequency are same in other word, when there is balance between wire feed speed and its melting rate.

**RELATIONSHIP BETWEN ARC EMISSIONS:**

Figure 15 show the relationship between infrared and acoustic rates where can be noticed that they have an inverse relation which means that when infrared rate increases, ignition rate (monitored by acoustic emission) decreases. Also is notices that when is greater the arc voltage, infrared rate is greater too and smaller is the ignition rate. This fact happens for all speed welding experiments. In all graphs also is possible to notice that when the arc voltage increases, the ignition rate variation, decreases and in all cases we can notice that the infrared rate has a low variation.

## 4. Conclusions

In the present work was approached the relationships between the weld bead geometry and arc emissions in GMAW-S process. After arc emission signals processing, it was found that both emissions reach a stationary state what means that they can be used as a monitor of welding process parameters. From acoustic emission was monitored short circuit rate, and was found that is possible to use this parameter for fit short circuits in GMAW-S process. By monitoring this parameter is possible to monitor the arc power which has an inverse relationship as well as it also has an inverse relationship with weld bead height and a direct relation with width weld bead. It was showed too that this parameter can monitor depth penetration and there are some arc voltage range where the responses has high stability (19-20 V).

Arc power and depth penetration was monitored satisfactory by infrared emission monitoring. It was noticed that there is a closed direct relationship between these parameters; high infrared rate, high depth penetration and so it possibilities to measure and monitor the dept penetration which is not trivial. Finally it was noticed that there is an inverse relationship between short circuit rate and infrared rate parameters which has sense because when the arc power increases the metal transfer rate also increases and the electrode wire consuming increases and the short circuit time cycle decreases and however its rate decreases. Welding speed and arc power influence arc sound as well as arc stability or metal transfer behaviour. The weld heat content reduces with welding speed. In this work, welding speed was found to affect the metal deposition, arc power and that acoustic and infrared emissions could be used for monitoring the weld bead geometry.

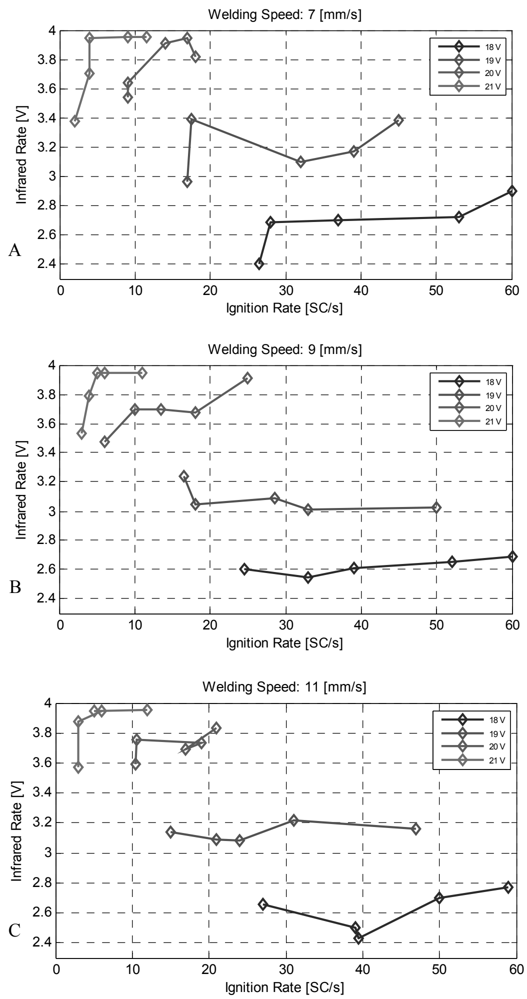


Fig. 15. Arc emissions

## Acknowledgements

The authors gratefully acknowledge support for this Project from The Brasilia University, the CNPq (Brazilian Research Council) and FINATEC (Private Research Foundation).

## References


[1] V. Kralj, Biocybernetic Investigations of hand movements of human operator in hand welding, The International Institute of Welding 68 (1968) 212-140.

[2] M. Drouet, F. Nadeau, Pressure waves due to arcing faults in a substation, IEEE Transactions On Power Application Systems 5 (1979) 98.

[3] Y. Arata, K. Inoue, M. Futamata, T. Toh, Investigation of welding arc sound (report 1) - effect of welding method and welding condition on welding arc sound, Transactions of Welding Research Institute Osaka University 8 (1979) 25-38.

[4] J. Tam, J. Huissoon, Developing psycho-acoustic experiments in gas metal arc welding, Proceedings of the International Conference on Mechatronics & Automation, Niagara Falls, ON, Canada, 2005,1112-1117.

[5] L. Grad, J. Grum, I. Polajnar, J. M. Slabe, Feasibility study of acoustic signals for on-line monitoring in short circuit gas metal arc welding, International Journal of Machine Tools and Manufacture 44/5 (2004) 555-561.

[6] E. H. Cayo, Monitoring, detection and localization system for welding defects based on the acoustic pressure of the GMAW-S process electric arc, Master Dissertation in Mechatronics Systems, FT University of Brasilia, DF, Brazil, 2008.

[7] H. C. Wikle III, S. Kottilingam, R. H. Zee, B. A. Chin, Infrared sensing techniques for penetration depth control of the submerged arc welding process. Journal of Materials Processing Technology 113 (2001) 228-233.

[8] G. E. Cook, J. E. Maxwell, R. J. Barnett and A. M. Strauss, Statistical process control application to weld process, IEEE Transactions on Industry Applications 33 (1997) 454-463.

[9] H. C. Wezenbeek, A System for Measurement and Control of Weld Pool Geometry in Automatic Arc Welding. Technische Univ.Eindhoven Netherlands, Departanent of Electrical Engineering. Eindhoven, The Netherlands, 1992.

[10] S.C. Absi Alfaro, G.C. Carvalho, F.R. da Cunha, A statistical approach for monitoring stochastic welding processes, Journal of Materials Processing Technology 175 (2006) 4-14.